Experimental Observation of a Peculiar Effect in Saturated Electron Paramagnetic Resonance Spectra Undergoing Spin Exchange. Magnetic Polariton?

Barney L. Bales[1], Miroslav Peric[1], Ileana Dragutan[2*], Michael K. Bowman[3], Marcel M. Bakirov[4], and Robert N. Schwartz[5]

[1] Department of Physics and Astronomy, California State University at Northridge, Northridge, CA, 91330, USA..
[2] Center of Organic Chemistry, Romanian Academy, 71141 Bucharest, Romania. Deceased.
[3] Department of Chemistry & Biochemistry, The University of Alabama, Box 870336, Tuscaloosa, AL, 35487 USA.
[4] Zavoisky-Physical-Technical Institute, FRC Kazan Scientific Center of RAS, Kazan 420029, Russian Federation. pinas1@yandex.ru
[5]Electrical and Computer Engineering Department, University of California, Los Angeles, Los Angeles, CA90095, USA.

Current email: barney.bales@csun.edu, miroslav.peric@csun.edu, mkbowman@retiree.ua.edu, pinas1@yandex.ru, rnschwartz@msn.com

* Shortly after finishing writing her part of this transcript, Ileana's husband informed us of the tragic, sudden death of our colleague and good friend. She will be missed by us and her many colleagues around the world.

Abstract

We report the experimental observation of a spectral manifestation of a magnetic polariton that was theoretically predicted last year. This unprecedented manifestation is demonstrated not only for ^{15}N-enriched peroxylamine disulfonate, a radical that adheres strictly to the assumptions of the theory, but also for a radical, 4-oxo-2,2,6,6-tetramethylpiperidine-d16;1-15N-1-oxyl, that departs somewhat from the assumptions, as well as the Galvinoxyl radical that represents a severe departure. The magnetic polariton is likely to be of interest to physical chemists in other fields because of the intrinsic advantage of a finite basis set in developing theories.

TOC Graphic

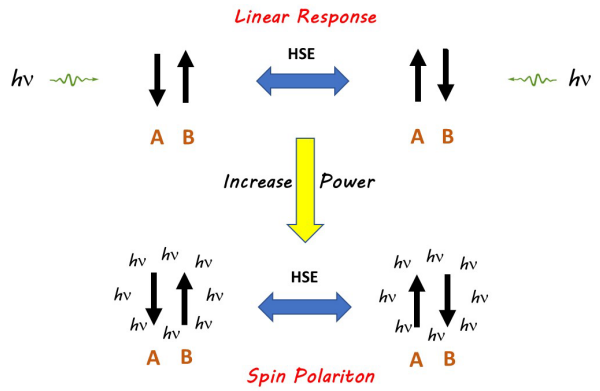

The title of this Letter was inspired by the first [1] of three papers by Salikhov [1-3] dealing with paramagnetic particles undergoing Heisenberg spin exchange (HSE) in liquids when the spectra are power saturated. The theories [1-3] treated a simplified EPR spectrum consisting of two identical Lorentzian EPR lines separated by A_{abs} with identical values of T_1 and T_2. A brief summary of Salikhov's principle findings is given in the Supplementary Information (SI). For a complete presentation of the modern view of spin exchange, see Salikhov's recent book [4].

For unsaturated spectra, HSE in liquids is a well-known phenomenon with a well-developed theory [5] and numerous applications [6]. Briefly, the changes in a well-resolved multiline EPR spectrum as HSE increases are as follows: for rates of HSE much less than A_0, the lines broaden and shift toward the center of the spectrum, for rates on the order of A_0, they merge, and for very high rates, the lines narrow into a single Lorentzian line. A_0 is the limit of the line separation A_{abs} as HSE $\rightarrow 0$ for unsaturated spectra. Perhaps less familiar to readers in other fields is the fact that transfer of spin coherence upon collision introduces a dispersion component described further below. The interested reader may consult ref. [5] and references therein for a recent review of the history and current understanding of the experiments. Also see ref. [7].

Saturation sets in when the circularly polarized magnetic induction of the microwave field, H_1, increases and the spin system leaves the linear-response regime. We restrict the discussion to radicals that tumble rapidly, producing motionally narrowed EPR. Spectra are presented as first derivatives. Of several peculiar effects discussed [3], we treat only one in this Letter: a predicted increase in A_{abs} as saturation increases, an effect that has not been observed experimentally. This effect is a hallmark of the various peculiar effects and for convenience call it the A_{abs} vs. H_1 effect (AHE). Salikhov proposed that the peculiar effects were a manifestation of the formation of collective modes between the spin system and the photons in strong H_1 fields and suggested the names magnetic or spin polaritons [2-3].

The rate of HSE is denoted by $V = K_{ex}C$, where K_{ex} is the rate constant of HSE, γ the gyromagnetic ratio of the electron, and C the radical concentration in moles/L. A_{abs} denotes the line separation for saturated spectra at any value of $C > 0$; $A_{abs}^0 = A_{abs}$ as $H_1 \rightarrow 0$; and $A_0 = A_{abs}^0$ as $C \rightarrow 0$. H_1 is proportional to $\sqrt{P}$, where P is the power of the microwave field.[8] See Table S1 of the SI for a summary of the important definitions and acronyms.

For unsaturated spectra in the presence of HSE, the two lines are spin modes that are collective states not representing a particular spin, each line is the sum of one absorption (ABS) and one HSE-induced dispersion signal (DIS). The existence of the DIS has been known since 1962 [9-11] being derived from perturbation theory for $V/\gamma A_0 << 1$, but it was not used to study HSE until 1997.[12] In 2003 it was first suggested [13] that only one ABS and one DIS were required over the entire range of $V/\gamma A_0$, a fact confirmed independently in refs [14] and [7] for unsaturated spectra. Thus, the restriction $V/\gamma A_0 << 1$ is not necessary. Here and elsewhere, [15] it has been shown experimentally that DIS begins to play a dominate role in the observed spectrum as V increases.

The peculiarities in refs [1-3] are only significant when the spectra are both saturated and V is significant. Despite a large experimental and theoretical literature on saturation and likewise on HSE, there have been very few experimental investigations where both phenomena were significant and none of those addressed the presence of DIS until this year.[16] No evidence of the AHE was uncovered in ref [16] because that investigation was limited to low values of both V and H_1.

Salikhov's theory [3] assumed (1) identical radicals yielding two identical Lorentzian lines and (2) that during one collision between a radical pair no re-encounters [17] occur. The predictions may be directly applied to ^{15}N nitroxide free radicals fulfilling (1) and (2). Rigorously, only ^{15}N-enriched peroxylamine disulfonate (15PADS) satisfies these restrictions because all other nitroxides have protons(deuterons) leading to inhomogeneous broadening, which violates (1). Furthermore, in all cases thus far studied, except for PADS, all nitroxides were found to re-encounter.[12-13, 18-20] Nevertheless, Salikhov[3] notes that, in practice, all ^{15}N nitroxides are expected to satisfy (1) when V is large compared with the hyperfine coupling constants due to protons (deuterons).

AHE is revealed in a continuous-wave saturation curve (CWS) where A_{abs} is plotted vs. H_1 Other spectral properties commonly treated theoretically and experimentally are the peak-to-peak line width of the ABS, ΔH_{pp}^{L}, and the peak-to-peak intensity of the ABS, V_{pp}. The doubly-integrated intensity of the spectrum, I may be derived from these quantities.[8] The CWS of the amplitude of the DIS, V_{disp}, was studied theoretically and experimentally for the first time earlier this year.[16] No theory prior to 2018 [16] predicted the AHE. See Figure 1 for definitions of the important parameters.

Because we wish to study first a radical that complies with the assumptions of the theory, our primary focus is on 15PADS. Counteracting the advantage of fulfilling the requisites of the theory are its limited solubility and absence of temperature dependence of V compared with uncharged nitroxides.[21] In the work described here, these two factors conspire to limit $V \approx \gamma A_0/2$, too small to collapse the two-line spectrum where some of the peculiarities that occur for $V \approx \gamma A_0$ [3]. Fortunately, the AHE is observable over a considerable range of $V < \gamma A_0$; therefore that is our focus.

In the recent paper,[16] which studied both HSE and saturation taking into account DIS, the theory predicted AHE; however, only as numerical results.[16] The exciting feature of ref [3] is that it provides analytical equations to describe the peculiar features of all of the measurable parameters. Our interest in the existence of a magnetic polariton is two-fold. Relative to the important area of polariton chemistry,[22] there is an inherent advantage provided by the finite basis sets in the theory of the magnetic polariton. The primary purpose of this paper is to demonstrate that AHE has been observed not only for 15PADS, but also for another nitroxide and, perhaps more significantly, for a radical that is very different from nitroxides and the limitations imposed in ref [3].

Figure 1a shows the EPR spectrum of 120-mM 15PADS in an air-saturated aqueous 50-mM K_2CO_3 solution at 295 K. The decompositions of the spectrum into the low- and high-field (lf and hf) ABS and DIS components are shown in **b** and **c**, respectively. This type of decomposition was first demonstrated in 1997[12] for unsaturated spectra where it was shown that V could be measured from ΔH_{pp}^{L} or the ratio V_{disp}/V_{pp}. It may also be measured from A_{abs} provided that the radicals do not re-encounter during one collision.[18] The behavior of unsaturated spectra undergoing HSE has been studied exhaustively experimentally; e.g.,[5] and theoretically.[4] In this work, values of V are obtained from ΔH_{pp}^{L} as detailed in the SI. Note that measuring any of the four parameters in Figure 1 requires decomposing the spectra; none of them is available directly from the spectrum itself. We achieve the decompositions by fitting the spectra employing the program Lowfit which is described in detail in the (SI) of ref [16]. Details of experimental procedures, spectral analysis, rationale for the selection of the radicals, and an example where the two lines have merged into one at $V/\gamma A_0 = 0.781$ may be found in the SI of this Letter.

Figure 1 is fit with a purely Lorentzian shape. Figure 1a shows that the residual (the difference between the spectrum (**a**) and the sum of (**b**) ABS and (**c**) DIS) is basically a flat line aside from very weak noise. The near perfect fit confirms that the lines are Lorentzian and that only one ABS and one DIS are required for each line under saturating conditions. Thus, this feature that holds for unsaturated spectra also holds for saturated spectra. The fits to all spectra in the CWS were excellent; only the featureless white noise in the residual becomes more evident as H_1 decreases. The Lorentzian shape describes the line shapes at all powers. Furthermore, for all CWS, only one DIS and one ABS for each line were needed. Extrapolation of A_{abs}^0 to V = 0 yielded A_0 = 18.24 ± 0.02 G which is in agreement with A_0 = 13.03 ± 0.03 G for 14PADS[23] after taking into account the ratio of the dipole moments, 1.403, of the ^{14}N vs ^{15}N isotopes.

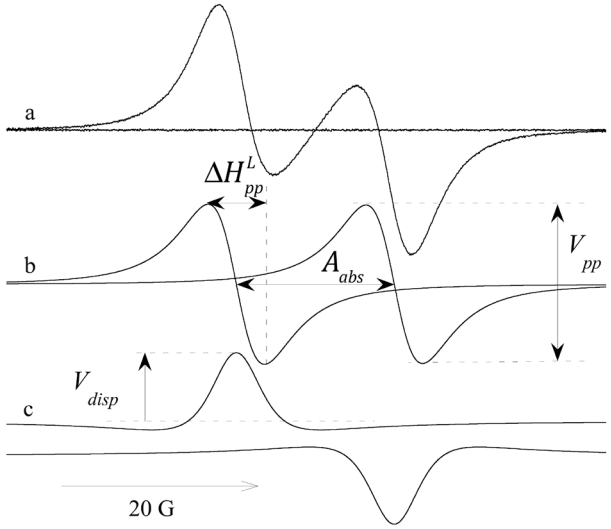

Figure. 1. (**a)** X-band EPR spectrum of 120-mM 15PADS at 295 K, (**b)** the ABS and (**c)** the DIS. The baseline shows the difference in spectrum **a** and the sum of **b** and **c**. P = 0.0631 W. The lf- and hf-DIS are displaced vertically for clarity. $V/\gamma A_0$ = 0.513 ± 0.005. Note that the spacing between where the spectrum crosses the baseline in spectrum **a** is significantly different from A_{abs}. There are no features in the spectrum that allow direct measurement of any of the four parameters without spectral fitting.

All CWS for C > 0.3 mM showed significant AHE, confirming this hallmark prediction of ref. [3]. For the spectrum of Figure 1, the CWS of A_{abs} is shown by the solid squares in Figure 2a accompanied by 4 others at lower concentrations. Note that the line shifts due to V are larger than those due to the AHE. Figure 2b displays the same data normalized to A_{abs}^0.

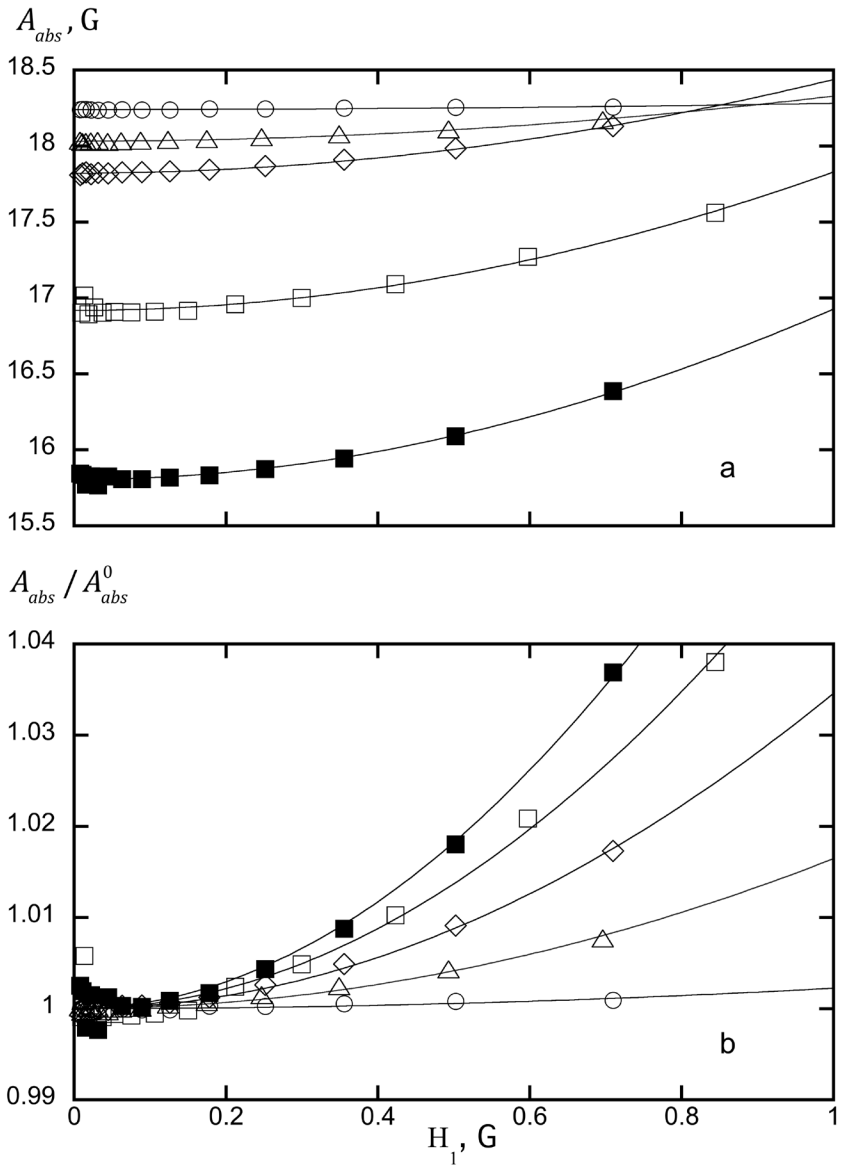

Figure 2. (a) Line shifts versus H_1; the intercepts yield values of A^0_{abs}. (b) Line shifts versus H_1 normalized to A^0_{abs}. For symbols, values of V/γ, and nominal concentrations, see Table 1. The solid lines are fits to eq 1. The fit errors are small compared with the size of the symbols.

The solid lines in Figure 2 are fits to eq. 1, an empirical equation inspired by the Bloch expression for the CWS ΔH^L_{pp}.[8] There is no theoretical basis for eq 1; however, as may be judged from Figure 2, good fits are obtained. We have found these to be useful in our preliminary comparisons of the experimental results and eq. 10 of ref. [3].

$$A_{abs}(V) = A^0_{abs}(V)[1 + H_1^2 S_{abs}(V)]^{1/2}, \quad (1)$$

Table 1. Parameters from Figure 2.

V/γ, G[a]	Symbol	A^0_{abs}, G[b]	$S_{abs}(V)$, G^{-2} [b,c]	C, mM

9.35 ± 0.03	Filled Squares	15.805 ± 0.007	0.147 ± 0.006	120
7.15 ± 0.02	Squares	16.918 ± 0.010	0.111 ± 0.006	92
3.93 ± 0.01	Diamonds	17.822 ± 0.002	0.070 ± 0.006	51
2.69 ± 0.01	Triangles	18.033 ± 0.002	0.0332 ± 0.0013	35
0.29 ± 0.01	Circles	18.241 ± 0.001	0.0045 ± 0.0006	3.7

[a] From eq S1 of the SI, error, sd from two lines. [b] Fit errors, eq 1. [c]Saturation parameter, eq 1.

Figure 2 confirms Salikhov's [3] predicted AHE for 15PADS. Importantly, we see that the phenomenon may be studied to good precision with a standard CW EPR having a 200-mW microwave source. Note that the magnetic polariton must be studied with a CW EPR spectrometer, which, as a practical matter, opens the door to experimental work in labs not equipped with pulsed spectrometers. It has occurred to us that interpreting some results from pulsed EPR experiments may have to be rethought in terms of the peculiar effects.

We now turn to brief experiments with two other radicals to show that the same phenomenon occurs even though they do not conform to the restricted assumptions of the theory. Figure 3a displays a spectrum and its decomposition of 30-mM 4-oxo-2,2,6,6-tetramethylpiperidine-d16;1-15N-1-oxyl (15PDT) (CDN isotopes) in decane at 295 K. The spectra in Figures 1 and 3 are rather similar despite the fact that the concentration of the latter is 4 times smaller. Figure 3b depicts the CWS of A_{abs} for 0.1 and 30-mM with the anticipated results: the former shows no shift with H_1 while the shift of the latter is significant. The intercept of A^0_{abs} yields A_0 = 20.090 ± 0.006 G. From eq S1 of the SI, we find that V/γ = 10.29 ± 0.02 G, so $V/\gamma A_0$ = 0.512. The solid line is the fit to eq 1, which is nearly as good as those for 15PADS in Figure 2.

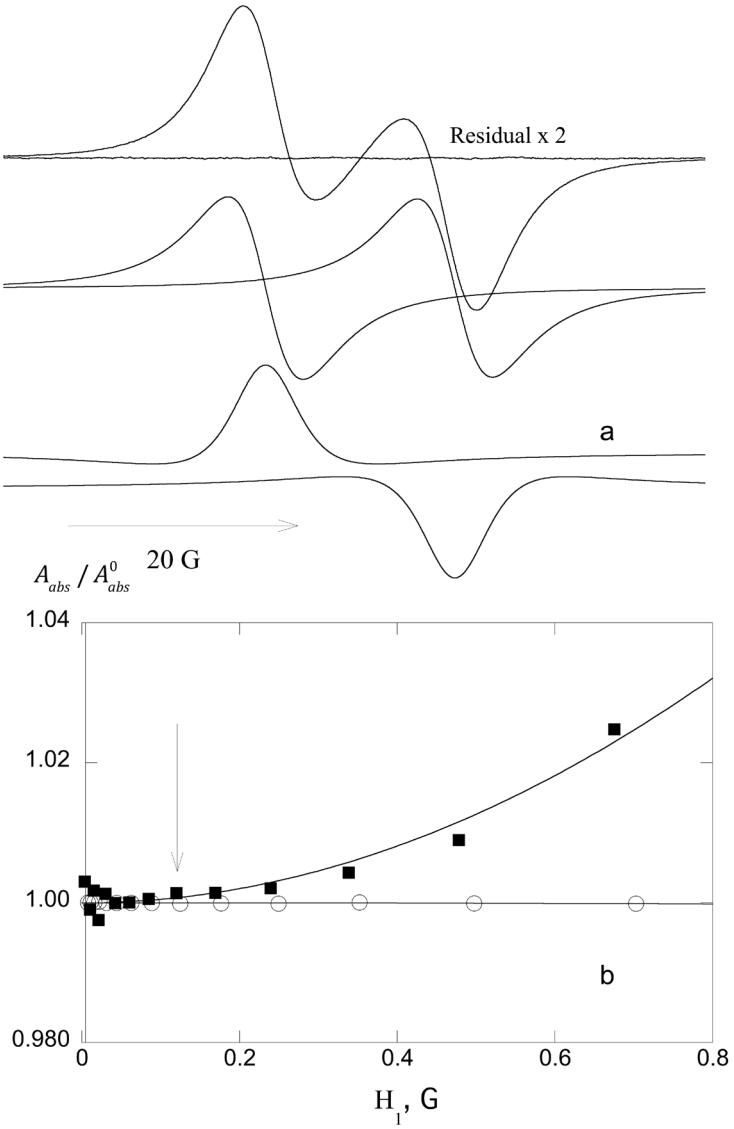

Figure 3. (**a)** X-band EPR spectrum of 30-mM 15PDT in decane at 295 K. P = 0.00631 W (H_1 = 0.120 G). Refer to Figure 1 for a description of the components and definitions of the parameters. The residual was multiplied by 2 so some noise could be observed. (**b)** The CWS of A_{abs}/A^0_{abs}: 30- and 0.1-mM, solid squares and circles, respectively. Solid line: fits to eq 1. The vertical arrow shows the datum from spectrum **a**.

For 15PDT, a strong dependence of K_{ex} on the temperature enables values of V sufficiently large to narrow the spectrum to a single Lorentzian line even for $C \leq 40$ mM. For example, a spectrum obtained from the same 30-mM at 340 K is displayed in Figure S4 of the SI, showing that the two-line spectrum has merged into a single line, although it is still composed of two spin modes that are easily separated by Lowfit. For other examples of the decomposition of merged single lines, see Figures 5 and 6 of ref [15] (experimental) and Figures 4, 5, and 9 of ref. [7] (simulated). To demonstrate AHE, values of $V/\gamma A_0$ leading to the merging of the lines are not needed as can be appreciated from the first panel of Figure 3 of ref [3]. However, merged spectra will need to be analyzed to test in depth other predictions of ref [3].

Finally, let us turn to Galvinoxyl radical (GALV) (Aldrich) whose room-temperature (RT) spectra are displayed for 0.1-mM, Figure 4a and 10 mM, 4**c.** There appear to be 9 lines in spectrum **a**; however, there are 10 because two of them overlap in the center. The ten lines consist of a pair of pentuplets due to the splitting by the 4 equivalent ring protons; the two pentuplets are split by the bridge proton coupling, A_{abs}. Each of the 10 lines is a multiplet of 37 overlapping hyperfine lines due to the 36 equivalent *t*-butyl protons. At a lower concentration, 0.01 mM (spectrum not shown), the 10 lines are well resolved and nearly Gaussian in shape, from which we measure A_0= 5.80 ± 0.04 G. As C (and therefore V) increases), the *t*-butyl patterns exchange narrow to form Lorentzian lines that overlap (Figure 4a) because all the lines broaden and the lines in each pentuplet move toward one another. With further increases in V, these ring proton lines shift toward one another and merge, yielding two lines, each consisting of 5 unresolved lines. Fitting each line of the doublet in Figure 4c to a Voigt line yields a Voigt parameter[24] $\chi \equiv \Delta H_{pp}^{G}/\Delta H_{pp}^{L}$ = 1.75 ± 0.01,[24] a large departure from Lorentzian. ΔH_{pp}^{G} is the Gaussian line width due to the unresolved hyperfine structure.[24] The fact that each of the two lines in Figure 4 is a Voigt attests to the fact that V is not sufficiently large to exchange-narrow the pentuplets. For the spectrum in Figure 4c, V/γ = 3.98 ± 0.05 G which yields $V/\gamma A_0$ = 0.67 ± 0.05. At higher concentrations (not shown) the entire spectrum narrows to a single line of Lorentzian shape. More details are available in the SI.

Thus, GALV is a radical that yields spectra very far removed from the assumptions of ref [3] but nevertheless presents a two-line spectrum. The decomposition of spectrum **c** into DIS and ABS for two values of P are displayed in Figure S5 of the SI. Figure 4d shows the CWS of A_{abs} for 0.01-mM and 10-mM samples. The solid lines are fits to equations of the form of eq 1. The broad two-line spectra in Figures 1, 2, and 4 are similar in appearance; however, line shapes of the first two are accurately Lorentzian while the third is not. The AHE with the available power of 200 mM show increases of a few percent for 15PADS and 15PDT while for Galvinoxyl, about 50%.

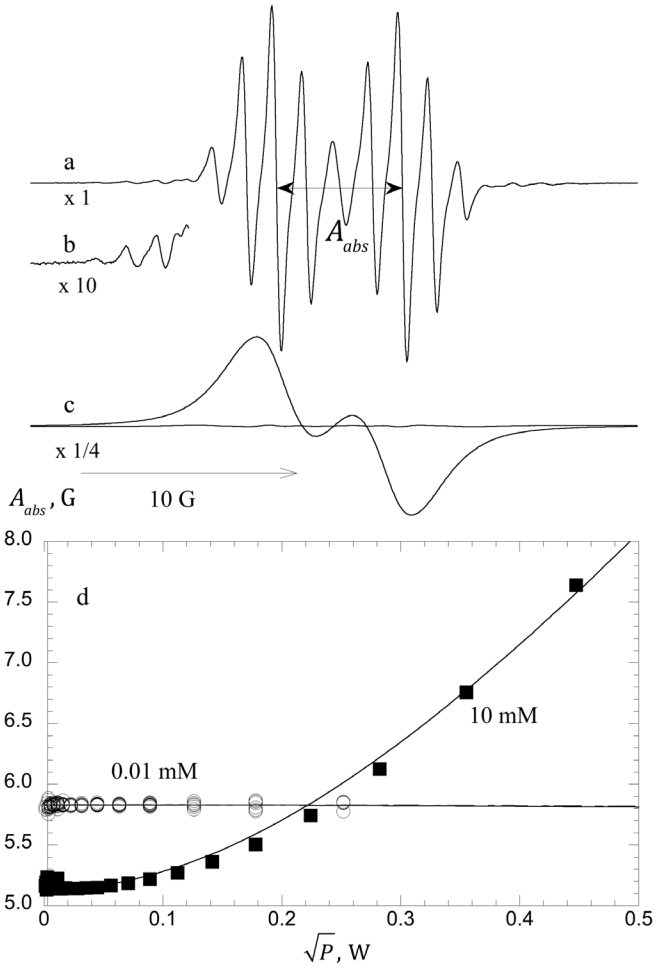

Figure 4. (**a)** X-band EPR spectrum of 0.1-mM Galvinoxyl in toluene at RT (292 K) at P = 0.0126 W. (**b)** Wing of spectrum **a** showing weak lines (x10) due to ^{13}C in natural abundance. (**c)** Spectrum with residual for 10-mM Galvinoxyl (x1/4) at P = 0.0126 W fit to only two pairs of Voigt lines. $V/\gamma A_0 = 0.67 \pm 0.05$. (**d)** CWS of A_{abs} for 0.01-mM, circles (spectrum not shown) and for 10-mM, solid squares. Solid lines: fits with an equation of the same form as eq 1 but with independent variable $\sqrt{P}$. The excellent fit of spectrum **c** is achieved with a Voigt shape rather than a Lorentzian. Note: for GALV, A_{abs} is a proton hyperfine spacing, not nitrogen.

We conclude that the AHE is readily observable in experiments with a system conforming to the theory, 15PADS, one that is not far removed from the theory, 15PDT, and even radicals with 370 lines, GALV. AHE can hardly be considered a special case unique to two-line systems. However, the two-line system provides an important model that can be readily solved and can provide valuable insights into much more complicated systems of interest.

This peculiar effect and the spin polariton underlying it are readily accessible to experiments at RT, using standard CW EPR spectrometers, modest microwave powers, and a wide variety of readily available free radicals. EPR provides convenient experimental access to a rather complicated polariton involving strongly interacting particles that are also strongly interacting with microwave photons.

It is intriguing that such an increase in A_{abs} has never been reported in the magnetic resonance literature even though countless experiments (including many in our labs) have been carried out under conditions conducive to its observation. Salikhov's[3] prediction piqued our interest, so with a bit of skepticism, we decided to see if we could detect the effect. There was no difficulty in corroborating the prediction in literally every system and sample we looked at.

The reader may wonder why this peculiar effect with its potential importance has escaped experimentalist's attention, so we offer our speculation on why this is the case. The effect is quite small for nitroxides and would be difficult to discover were it not for the increased precision afforded by spectral fitting and extraordinary field-sweep accuracy and linearity in modern commercial spectrometers. One cannot simply "notice" the increase in A_{abs} in spectra such as these; it must be uncovered by spectral decomposition. This may be appreciated visually in Figure S5 of the SI, which clearly shows that the ABS lines shift outward with P while the spectral lines do not.

What is next? Our first focus will be on 15PADS carrying out further experiments and comparing with theory, not only for A_{abs}, but also for ΔH_{pp}^{L}, V_{disp}/V_{pp}, and I, which are shown up to H_1 = 2 G in Figures 3, 5, and 6, of ref [3], respectively. When contemplating these figures, we suggest that the reader keep in mind that only $H_1 \approx 1$ G is achievable for many commercial spectrometers. There are analytical expressions for these quantities in ref [3]; see Table S1 of the SI for a brief description of the predicted results, which shows that there are interesting behaviors of all four parameters some of which may be studied at the modest values of $V/\gamma A_0$ accessible with 15PADS. For us, the most interesting is V_{disp}/V_{pp} because almost nothing is known.[16]

Peculiar features that occur when the spectra collapse, A_{abs} = 0, for $V = V^*$are not accessible with 15PADS, therefore, we shall study 15PDT to higher values of $V/\gamma A_0$. The analytical expressions in ref [3] are still valid at V^* and above. To be rigorous, the re-encounter mechanism must be added to the theory. A simple starting point to explore the peculiar effects will be to determine the value of V^* from A_{abs}, V_{disp}/V_{pp}, and ΔH_{pp}^{L}. The theory[3] predicts that V^* is dependent on H_1 and should be the same as determined from these three parameters.

Finally, GALV offers a stringent test of our understanding of inhomogeneously broadened spin modes under saturation. There is little chance that analytical equations will be obtained; however, theories exist[4, 16] that, either in their present form or by adding relaxation mechanisms, could simulate spectra even for radicals even more complex than GALV. In such work, we envision that programs such as Lowfit would be applied to both theoretical and experimental spectra to provide comparisons.

We close with a quote from 45 years ago by the editors of a volume[25] dedicated to the at-that-time relatively new technique of CIDEP: "Magnetic resonance has constantly been able to surprise with its ability to exhibit new phenomena. Just when it appears to be entering a quiet middle age it bursts into activity with some new manifestation of its versatility." Salikhov[1-3] has proposed new phenomena, one of which has now been observed experimentally. Will the magnetic polariton blossom into something important?

Acknowledgments

M.P. gratefully acknowledges support from NSF RUI (grant no. 1856746). M.M.B. acknowledges financial support from the government assignment for FRC Kazan Scientific Center of RAS.

Supporting information is available free of charge at https:// etc

Summary of definitions and acronyms.
Summary of Theoretical Findings
Choice of Radicals
Synthesis of 15PADS
CW EPR
Further experimental details
Spectral Analysis
Example of a merged 15PDT Spectrum
To study AHE, the spectra must be decomposed when the lines severely overlap
SI references

References

1. Salikhov, K. M., Peculiar Features of the Spectrum Saturation Effect When the Spectral Diffusion Operates: System with Two Frequencies. *Appl. Magn. Reson.* **2018,** *49*, 1074 - 1087.
2. Salikhov, K. M., New paradigm of spin exchange and its manifestations in EPR. *Appl. Magn. Reson.* **2020,** *51*, 297-325.
3. Salikhov, K. M., New Information About Manifestations of Spin Exchange in the EPR Spectra of Solutions of Paramagnetic Particles Under Saturation Conditions. *Appl. Magn. Reson.* **2021,** *52*, 1063-1091.
4. Salikhov, K. M., *Fundamentals of Spin Exchange. Story of a Paradigm Shift*. Springer: Switzerland, 2019; p 265.
5. Bales, B. L.; Bakirov, M. M.; Galeev, R. T.; Kirilyuk, I. A.; Kokorin, A. I.; Salikhov, K. M., The Current State of Measuring Bimolecular Spin Exchange Rates by the EPR Spectral Manifestations of the Exchange and Dipole-dipole interactions in Dilute Solutions of Nitroxide Free Radicals with Proton Hyperfine Structure. *Appl. Magn. Reson.* **2017,** *48*, 1399-1445.
6. Marsh, D., *Spin-Label Electron Paramagnetic Resonance Spectroscopy*. CRC Press. Taylor & Francis Group: Boca Raton, FL. USA, 2020; p 495.
7. Bales, B. L.; Peric, M., EPR Line Shifts and Line Shape Changes Due to Spin Exchange Between Nitroxide Free Radicals in Liquids 10. Spin-Exchange Frequencies of the Order of the Nitrogen Hyperfine Interaction: A Hypothesis. *Appl. Magn. Reson.* **2017,** *48* (2), 175-200.
8. Bakirov, M. M.; Salikhov, K. M.; Peric , M.; Schwartz, R. N.; Bales, B. L., A Simple, Accurate Method to Determine the Effective Value of the Magnetic Induction of the Microwave Field from the Continuous Saturation of EPR Spectra of Fremy's Salt Solutions. Representative values of T_1. *Appl. Magn. Reson.* **2019,** *50*, 919-942.
9. Currin, J. D., Theory of Exchange Relaxation of Hyperfine Structure in Electron Spin Resonance. *Phys. Rev.* **1962,** *126*, 1995.
10. Kivelson, D.; Ogan, K., Spin Relaxation in Terms of Mori's Formalism. In *Advances in Magnetic Resonance*, Waugh, J. S., Ed. Academic Press: New York, 1974; Vol. 7, pp 71-155.
11. Molin, Y. N.; Salikhov, K. M.; Zamaraev, K. I., *Spin Exchange. Principles and Applications in Chemistry and Biology*. Springer-Verlag: New York, 1980; Vol. 8, p 242.
12. Bales, B. L.; Peric, M., EPR Line Shifts and Line Shape Changes Due to Spin Exchange of Nitroxide Free Radicals in liquids. *J. Phys. Chem. B* **1997,** *101*, 8707-8716.

13. Bales, B. L.; Peric, M.; Dragutan, I., EPR Line Shifts and Line Shape Changes Due to Spin Exchange of Nitroxide Free Radicals in Liquids 3. Extension to Five Hyperfine Lines. Additional Line Shifts Due to Re-encounters. *J. Phys. Chem. A* **2003,** *107*, 9086-9098.
14. Salikhov, K. M., Consistent Paradigm of the Spectra Decomposition into Independent Resonance Lines. *Appl. Magn. Reson.* **2016,** *47*, 1207 - 1227.
15. Bales, B. L.; Peric, M., EPR Line Shifts and Line Shape Changes Due to Spin Exchange of Nitroxide Free Radicals in Liquids 2. Extension to High Spin Exchange Frequencies and Inhomogeneously Broadened Spectra. *J. Phys. Chem. A* **2002,** *106*, 4846-4854.
16. Bakirov, M. M.; Khairuzhdinov, I. T.; Salikhov, K. M.; Schwartz, R. N.; Bales, B. L., The Effect of Power Saturation on the Line Shapes of Nitroxide Spin Probes Under the Influence of Spin-Exchange and Dipole–Dipole Interactions Studied by CW EPR. *Appl. Magn. Reson.* **2022,** *53*, 1275-1350.
17. Salikhov, K. M., The Contribution from Exchange interaction to Line Shifts in ESR Spectra of Paramagnetic Particles in Solutions. *J. Magn. Reson.* **1985,** *63*, 271-279.
18. Bales, B. L.; Meyer, M.; Smith, S.; Peric, M., EPR Line Shifts and Line Shape Changes Due to Spin Exchange of Nitroxide-Free Radicals in Liquids 4. Test of a Method to Measure Re-encounter Rates in Liquids Employing ^{15}N and ^{14}N Nitroxide Spin Probes. *J. Phys. Chem. A* **2008,** *112*, 2177-2181.
19. Kurban, M. R.; Peric, M.; Bales, B. L., Nitroxide spin exchange due to re-encounter collisions in a series of *n*-alkanes. *J. Chem. Phys.* **2008,** *129*, 064501-1 - 064501-10.
20. Bales, B. L.; Harris, F. L.; Peric, M.; Peric, M., EPR Line Shifts and Line Shape Changes Due to Spin Exchange of Nitroxide-Free Radicals in Liquids 7. Singly Charged Surfactant Nitroxide. *J. Phys. Chem. A* **2009,** *113*, 9295-9303.
21. Eastman, M. P.; Bruno, G. V.; Freed, J. H., Studies of Heisenberg Spin Exchange. II. Effects of Radical Charge and Size. *J. Chem. Phys.* **1970,** *52*, 2511.
22. Ribeiro, R. F.; Martínez-Martínez, L. S.; Du, M.; Campos-Gonzalez-Angulo, J.; Yuen-Zhou, J., Polariton chemistry: controlling molecular dynamics with optical cavities. *Chem. Sci.* **2018,** *9*, 6325-6339.
23. Jones, M. T., Electron Spin Exchange in Aqueous Solutions of $K_2(SO_3)_2NO$. *J. Chem. Phys.* **1963,** *38*, 2892-2895.
24. Bales, B. L., Inhomogeneously Broadened Spin-Label Spectra. In *Biological Magnetic Resonance*, Berliner, L. J.; Reuben, J., Eds. Plenum: New York, 1989; Vol. 8, pp 77-130.
25. Muus, L. T.; Atkins, P. W.; McLaughlin, K. A.; Pedersen, J. S., *Chemically Induced Magnetic Polarization*. D. Reidel: Boston, 1977; Vol. 34, p 407.

Supplemental Information

Experimental Observation of a Peculiar Effect in Saturated Electron Paramagnetic Resonance Spectra Undergoing Spin Exchange. Magnetic Polariton?

Barney L. Bales, Miroslav Peric, Ileana Dragutan, Michael K. Bowman, Marcel M. Bakirov, and Robert N. Schwartz

Summary of definitions and acronyms.

Table S1 Definitions and Acronyms

HSE	Heisenberg spin exchange
CWS	Continuous wave saturation
K_{ex}	Rate constant of HSE ($M^{-1}s^{-1}$)
C	Molar concentration of the radical
$V = K_{ex}C$	Rate of HSE (s^{-1})
ABS	Absorption component of a superimposed absorption and dispersion line
DISP	Dispersion component of a superimposed absorption and dispersion line
P	Microwave power.
H_1	Circularly polarized magnetic induction of the microwave field; $H_1 \propto \sqrt{P}$.
V^*	Rate of HSE where the spectrum collapses to a single Lorentzian line, $A_{abs} \rightarrow 0$, above which two Lorentzian lines of different widths and intensities are predicted.
$V^{\otimes}$	Rate of HSE where V_{disp}/V_{pp} is independent of H_1.
A_0	Separation (G) of two unsaturated ABS lines as $C \rightarrow 0$.
A_{abs}^0	Separation (G) of two saturated ABS lines as $H_1 \rightarrow 0$.
A_{abs}	Separation (G) of two saturated ABS lines for $H_1 > 0$ and $C > 0$. Figure 1.
AHE	The hitherto unobserved effect of the increase in A_{abs} with H_1.
ΔH_{pp}^L	The peak-to-peak line width (G) of the ABS. Figure 1.
V_{disp}	The peak-to-peak height of the DIS. Figure 1.
V_{pp}	The peak-to-peak height of the ABS. Figure 1.
I	The doubly-integrated intensity of the ABS.

Summary of Theoretical Findings

Salikhov [1] generally suggests that T_1 and T_2 well as other parameters could be measured independently under saturation allowing comparison with low microwave field measurements. He details the behavior of A_{abs}, V_{disp}/V_{pp}, ΔH_{pp}^L, and I for significant values of $V/\gamma A_0$ under saturating conditions. Notable peculiar features are given in Table S2. Denote the value of V where the entire spectrum collapses into a single Lorentzian line as V^*. Denote by $V^{\otimes} < V^*$ the rate of HSE where no variation of V_{disp}/V_{pp} with H_1 is predicted. Figure 3 (right) in ref [1]

Table S2 Behavior of EPR Parameters

	Notable peculiar features	Figure in ref [1]
A_{abs}	1. For $V < V^*$, A_{abs} increases with V, the AHE. 2. The value of V^* increases with H_1.	Figure 3 (left)

V_{disp}/V_{pp}	1. For $V < V^{\otimes}$, V_{disp}/V_{pp} increases with V. 2. At $V = V^{\otimes}$, no variation with H_1 is predicted. 3. For $V > V^{\otimes}$ this ratio decreases with H_1.	Figure 5
ΔH_{pp}^{L}	1. For $V < V^{*}$, ΔH_{pp}^{L} increases with V and H_1 to V^{*} 2. At $V = V^{*}$, there is a discontinuity in the slope of ΔH_{pp}^{L} with respect to V. 3. For $H_1 \rightarrow 0$, the increase is linear; for larger values there is an initial non-linear increase followed by an approach to linear values at larger values of V. These limiting slopes are the same for all H_1 4. For $V > V^{*}$ two superimposed Lorentzian lines are predicted of different line widths. 5. The values of V^{*} are the same as those for A_{abs}.	Figure 3 (right)
I	1. For $V \rightarrow 0$, the CWS of I approaches a plateau as a function of H_1 as predicted by the Bloch equations. 2. For $V > 0 > V^{*}$, the CWS of I goes through a maximum. 3. For $V > V^{*}$, the narrower line has $I > 0$ while the broader has $I < 0$. These two lines were predicted a long time ago [2] for $H_1 \rightarrow 0$ but never been observed experimentally.	Figure 6

Choice of Radicals

15PADS, Figure S1, yields two equally intense lines from the ^{15}N hyperfine splitting at all concentrations. The spectrum in Figure 1, at C = 120 mM, is at the maximum value of V attainable due to limited solubility and limited temperature dependence of V. At low concentrations, the two lines are narrow: ΔH_{pp}^{L} = 0.14 G [3]. The low natural abundance of the only other magnetic nuclei, ^{33}S and ^{17}O, contribute negligibly to the spectra [3]. 15PADS is dianion, so radical-radical collisions are brief and multiple encounters within the spin relaxation time are rare [4].

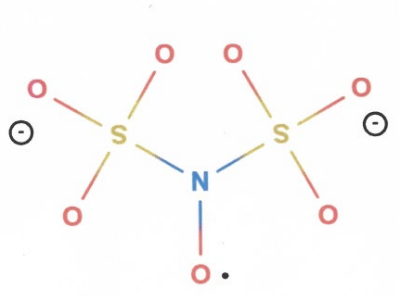

Figure S1 PADS dianion radical. 15PADS is enriched in ^{15}N. The only other magnetic nuclei, ^{33}S and ^{17}O, are present in negligible natural abundances.

15PDT, Figure S2, is a widely-used nitroxide free radical [5-8] that was chosen to relax the assumption of the theoretical treatment of two Lorentzian lines. The spectrum is composed of two equal-intensity multiplets of 25 lines separated by a scant $A_{abs}^{CD_3}$ = 0.017 G. Note that $A_{abs}^{H_{Ring}}$ = 0.003G for the 4 ring deuterons is negligible [9]. This radical deviates slightly from the

assumption that the two lines are Lorentzian. It is similar in size to 15PADS, but uncharged so both collisions and re-encounters are more frequent and vary strongly with temperature, e.g., Figure 5 of ref [10]. The same is true for all other nitroxides studied to date [4, 11-14].

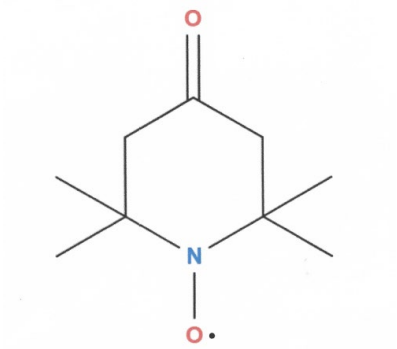

Figure S2 Tempone radical. 15PDT is enriched in ^{15}N and ^{2}H. The 12 methyl deuterons are equivalent with $A_{abs}^{CD_3}$ = 0.017 G and the hyperfine coupling to the ring deuterons is negligible, $A_{abs}^{H_{Ring}}$ = 0.003G [9].

GALV, Figure S3. The Galvinoxyl (Coppinger's) radical contains multiple protons, similar to many organic free radicals. The EPR spectrum is a doublet of pentuplets spaced by $A_{abs}^{H_{Bridge}}$ = 5.80 ± 0.05 G, this work. The pentuplets are formed by the 4 equivalent ring protons with $A_{abs}^{H_{Ring}}$ = 1.34 ± 0.01 G ENDOR [15], with the two center lines strongly overlapped to give 9 well-resolved lines. In addition, there are 36 equivalent *t*-butyl protons giving unresolved splittings due to the small $A_{abs}^{CH_3}$ = 0.050 ± 0.005 G ENDOR [15], giving a total of 370 lines. Additional lines from radicals containing ^{13}C in natural abundance are readily observable in the wings of the spectrum and more lines from of ^{2}H in natural abundance are to be expected. The GALV spectra reveal to what extent the spin polariton is restricted to two Lorentzian lines.

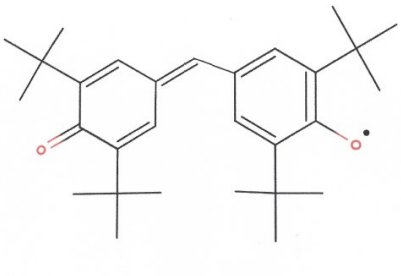

Figure S3 Galvinoxyl radical. The 36 methyl protons are equivalent with $A_{abs}^{CH_3}$ = 0.050 ± 0.005 G as are the four ring protons with $A_{abs}^{H_{Ring}}$ = 1.34 ± 0.01 G. The coupling constant of the bridge proton $A_{abs}^{H_{Bridge}}$ = 5.80 ± 0.05 G.

Synthesis of 15PADS

Several EPR studies make use of 15PADS [3, 16-19] yet its synthesis is reported to date either as an "in-house synthesis" [16-17, 19] or as proceeding through the electrolytic one-electron oxidation of the corresponding ^{15}N-hydroxylaminedisulfonate [18].

In this work, it was synthesized by adapting, with some modifications, the procedures published earlier [20-21] for ^{14}N-PADS. A solution of sodium bicarbonate (1.45 g; 17.26 mM) and 15N sodium nitrite (1.2 g; 17.14 mM; CDN Isotopes, Canada) in distilled water (25 ml) in a beaker cooled to - 5 °C in an ice-salt bath, was vigorously stirred, followed by continuous stirring while gaseous sulfur dioxide was bubbled through the solution at such a rate that the temperature was maintained between 0 – 5 °C. After ten minutes, the solution turned brownish but the color gradually disappeared on admission of SO_2 for another15 min. The cooling and introduction of SO_2 were discontinued and the stirred solution was allowed to slowly warm to 15 °C. At this point, the pH of the solution was 2, so argon was passed through to remove the excess SO_2. After 10 min, the solution was still strongly acidic, therefore 7 – 8 drops of a saturated solution of sodium carbonate were used to adjust the pH to 9. Then, under stirring at 6 – 15 °C, a solution of potassium permanganate (0.9 g; 5.7 mM) in 25 ml of water was added dropwise over 25 min resulting in a massive precipitation of manganese dioxide. Stirring was maintained for 40 min, the precipitate was filtered under a moderate vacuum, and the deep-violet filtrate was poured over solid potassium acetate (10 g) to spontaneously yield the intense yellow needles of ^{15}N-PADS in the dimerized form. After filtration under vacuum through a Büchner funnel, the salt was rapidly washed successively with a 20% solution of potassium acetate (10 ml; pH 11 following the addition of a few drops of 29% ammonium hydroxide), anhydrous ethanol (8 ml), dry acetone (8 ml) and ethyl ether (dried over a sodium wire; 2 x 8 ml). The still-wet crystals were collected from the funnel, placed into a Schlenk tube connected to a vacuum pump, and left to dry under vacuum for 3 – 4 h after which the Schlenk tube was tightly closed and weighed. 3.45 g (74.8 % yield) of the targeted dimer of the ^{15}N-PADS were obtained. When stored in the freezer in a Schlenk tube under a high vacuum, the salt is stable indefinitely [21].

CW EPR

CWS spectra for 15PADS and 15PDT were obtained in Northridge using the 2D-Field-Power routine in Bruker's Xenon software package at typically 13 – 15 power settings. As mentioned in the text, the conversion from power, P, to the magnetic induction of the microwave field, $H_1 = \Gamma\sqrt{Q}\sqrt{P}$, was carried out for the Northridge spectrometer using a standard sample of 14PADS as detailed in [22] where Q is the Q-value of the cavity and Γ is a constant pertinent to the sample and cavity configurations taking into account microwave focusing effects of the glassware. The Bruker set up affords straightforward measurement of Q; however, only to 2 significant figures, contributing to the experimental uncertainty in the determination of S_{abs}. Another quite significant source of error stems from the method of [22] because the calibration is based the value of T_1 determined by Kooser et al. [23] who estimated the uncertainty at 20 – 30 %. In addition to this uncertainty, we estimate that the *relative* values of H_1 are accurate to ± 4 % in any one run where the sample is left undisturbed; however, from run to run the precision is dominated by the uncertainty in Q. These uncertainties will be paramount when we compare our results with the analytical expressions in ref [1]. Here, the interest is in the observation of the magnetic polariton.

Further experimental details

An aqueous solution of 15PADS was prepared by weight at a nominal concentration of 139 mM in 50-mM K_2CO_3. The purity of 15PADS was determined to be 87 % by comparing its doubly-integrated intensity with that of a freshly prepared solution of 14PDT in 50-mM K_2CO_3,

thus yielding a nominal concentration of 120 mM. Another 15PADS solution was prepared to a concentration of 92 mM which was diluted to yield 34 mM. Then, 51- and 3.7-mM samples were obtained by heat annealing [4, 22] the 92-mM sample. These air-saturated solutions were drawn by capillary action into 5-μL disposable pipettes (id 0.3 mm) which were sealed at each end with Sigillum Wax Sealant (Globe Scientific 51601), inserted into a 3-mm NMR tube (Wilmad), and placed into the quartz dewar insert of the Bruker N_2 temperature controller. With the small bore of the 5-μL pipette we were able to obtain Q values on the order of 6500 – 7500 increasing the attainable values of H_1 over previous work [24].

15PDT Samples were drawn into open-ended polytetrafluoroethylene tubing with a Drummond Captrol II Microdispenser (PTFE - ID: AWG21) obtained from Zeus. The tubing was then folded in half, and the open ends were sealed with Seal-Ease plastic clay from Clay Adams, Inc. The tubing, folded end down, was then placed into a quartz tube made by Wilmad Glass Co, with a hole in the bottom. Finally, the quartz tube was inserted in the quartz dewar insert of a Bruker N_2 temperature controller. In this arrangement, N_2 was used to control the sample temperature and displace the oxygen, reducing the line width [25]. Plots of ΔH_{pp}^L versus N_2 flow time show that after 37 min, its change is < 1%. Here, because of the relatively small microwave loss of decane, we obtained Q-values 4700 – 5300 despite the larger extension into the microwave electric field region due to the larger physical dimensions of the sample.

GALV samples were prepared in toluene by weight and serial dilution from Galvinoxyl Radical (Aldrich), introduced into 4-mm O.D. quartz tubes and rigorously degassed with several freeze-pump-thaw cycles and flame sealed. Due to a noticeable loss of solvent during degassing, the concentrations are nominal. Spectra were obtained with a Bruker Elexsys E540 (Billerica, MA) employing 100 kHz magnetic field modulation with 0.1 G amplitude. This spectrometer has not yet been calibrated to give the proportionality constant of H_1 to $\sqrt{P}$.

Spectral Analysis

The rate of exchange V could be measured in three ways: (a) from broadening of the ABS lines; (b) from the relative heights of the DIS and ABS; and (c) from the decrease of A_{abs} at $H_1 \to 0$. This behavior of unsaturated spectra undergoing HSE is well-known experimentally, e.g., [26] and theoretically [27]. Each approach to measure V requires fitting for accuracy; none of the 3 parameters in Figure 1 are available directly from the spectrum. We achieve the decompositions by fitting the spectra employing the program Lowfit which is described in detail in the Supplemental Information (SI) of ref. [24]. Although V may be obtained from three sources, the precision of those from line broadening are significantly more precise. From ΔH_{pp}^L, V is obtained from the following, e.g., eq. 9b of ref. [28]:

$$V = \sqrt{3\gamma}\left[\Delta H_{pp}^L(C)_0 - \Delta H_{pp}^L(0)_0\right] \tag{S1}$$

where the subscript 0 means the limit when $H_1 \to 0$. Two values of ΔH_{pp}^L are available from the lf and hf.

Note that because each DIS is an odd function of the frequency (magnetic field) its doubly-integrate intensity (I) each of the two DIS is zero. Furthermore, because the two DIS are equal but of opposite signs, I would be zero for any function. The different symmetries of the ABS and DIS components mean that their superposition, which forms the spectrum, does not have a clearly identified feature at the center. Neither the centroid of the extrema nor the zero

crossing coincides with the center of the EPR line. This is particularly true when the spectral lines strongly overlap, but the lines have not collapsed into a single line, Figure S4. Although the EPR spectrum in Figure S4 appears to be a single line, it is the overlap of two unresolved lines which can nevertheless be revealed by fitting. The splitting A_{abs} is non-zero and non-negligible and the CW-EPR spectrum has its dominant contribution from the DIS components.

Figures 1, 3, and S4 expose a great danger in trying to doubly-integrate an experimental spectrum to obtain I. The DIS contributes nothing to I in theory but in practice with a finite sweep width, the DIS would erroneously contribute to I. The fact that the two DIS are equal and of opposite sign does mitigate this problem somewhat. Lowfit solves this problem to high precision by separating ABS and DIS and obtaining I from only the ABS.

Example of a merged 15PDT Spectrum

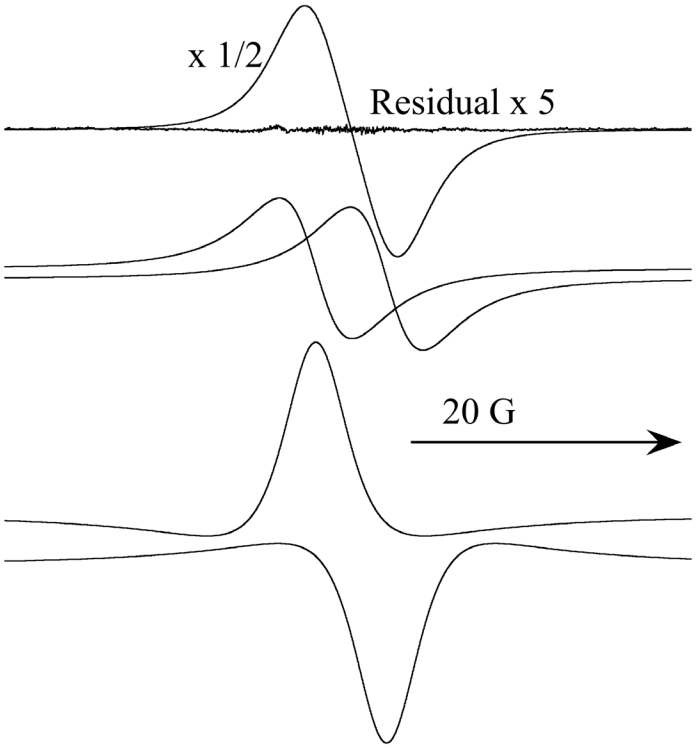

Figure S4. X-band EPR spectrum and decomposition of 0.030-M 15PDT in decane at 340 K illustrating the dominance of DIS at $V/\gamma A_0$ = 0.781. Refer to Figure 1 in the text for a description of the components and definitions of the parameters. The residual was multiplied by 5 so some noise could be observed.

To study AHE, the spectra must be decomposed when the lines severely overlap

Figure S5 illustrates the need to decompose the spectra into their ABS and DIS components to study the AHE when the lines overlap. While the value of A_{abs} properly measured from the decomposed components (either ABS or DIS), increases with power, the apparent separation of the undecomposed spectra does not. At lower values of V where the lines do not overlap significantly, the effect is noticeable. Nevertheless, even though the effect is

noticeable, decomposition is paramount in order to separate the ABS and DIS because the crossing points are not equal to A_{abs}.

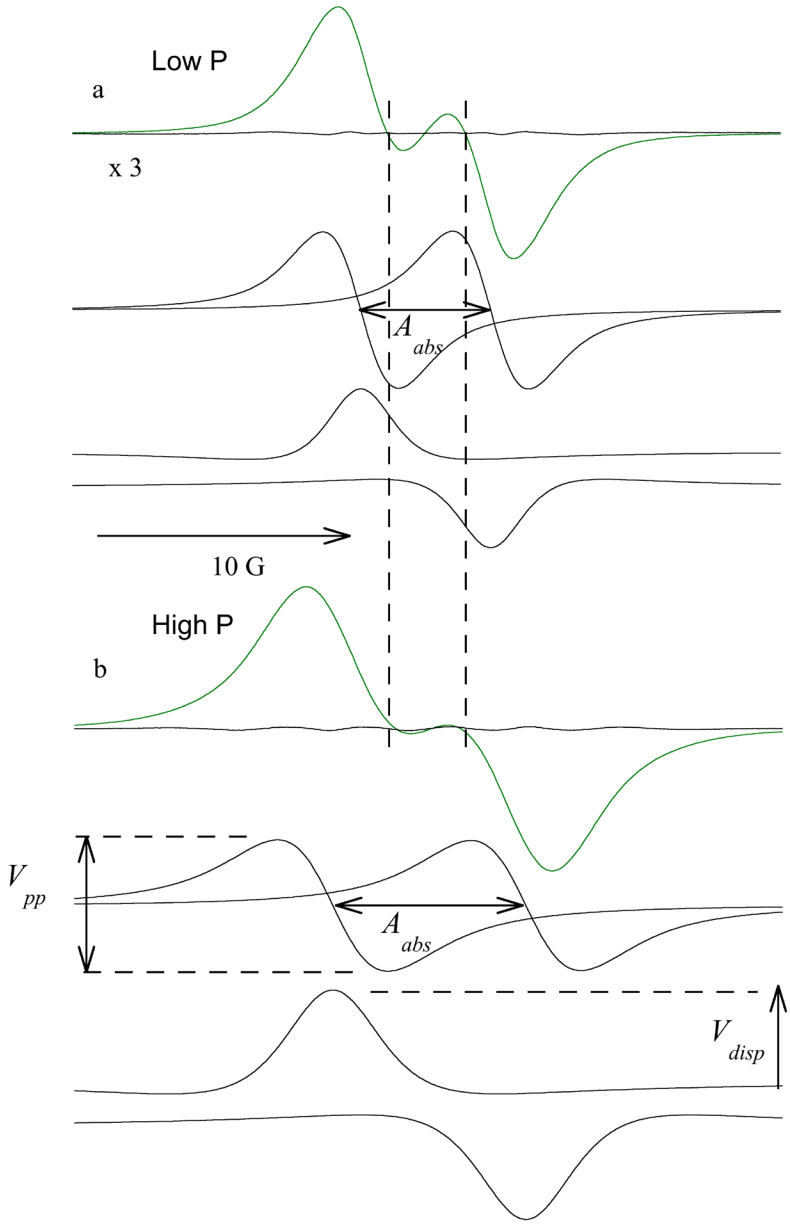

Figure S5. GALV spectra and their decompositions are shown in, **a**, P = 0.795 mW and **b**, = 200 mW. From the separation of the decomposed lines, either ABS or DIS, labeled A_{abs}, we see that this separation is larger at high power, clearly verifying the AHE. On the other hand, trying to discern the AHE from the spectra themselves (in green) is futile. We see that the separation of the crossing points of the spectra, shown by vertical dashed lines, do not increase; in fact, they become slightly smaller at higher power.

1. Salikhov, K. M., New Information About Manifestations of Spin Exchange in the EPR Spectra of Solutions of Paramagnetic Particles Under Saturation Conditions. *Appl. Magn. Reson.* **2021,** *52*, 1063-1091.
2. Kivelson, D.; Ogan, K., Spin Relaxation in Terms of Mori's Formalism. In *Advances in Magnetic Resonance*, Waugh, J. S., Ed. Academic Press: New York, 1974; Vol. 7, pp 71-155.
3. Okazaki, M.; Toriyama, K., Ultra High-Resolution ESR Using a Reverse Micelle ^{33}S, ^{17}O, and ^{15}N Satellite Lines of Fremy's Salt at Natural Isotopic Abundance. *J. Magn. Reson.* **1988,** *79*, 158-162.
4. Bales, B. L.; Peric, M., EPR Line Shifts and Line Shape Changes Due to Spin Exchange of Nitroxide Free Radicals in liquids. *J. Phys. Chem. B* **1997,** *101*, 8707-8716.
5. Berliner, L. J., *Spin Labeling II: Theory and Applications*. Academic Press: New York, 1979.
6. Berliner, L. J., *Spin Labeling: Theory and Applications*. Plenum Publishing Corporation: New York, 1989; Vol. 8.
7. Berliner, L. J., *Spin Labeling: The Next Millennium*. Kluwer Academic Publishers: New York, Boston, Dordrecht, London, Moscow, 2002; Vol. 14, p 444.
8. Marsh, D., *Spin-Label Electron Paramagnetic Resonance Spectroscopy*. CRC Press. Taylor & Francis Group: Boca Raton, FL. USA, 2020; p 495.
9. Bales, B. L., Inhomogeneously Broadened Spin-Label Spectra. In *Biological Magnetic Resonance*, Berliner, L. J.; Reuben, J., Eds. Plenum: New York, 1989; Vol. 8, pp 77-130.
10. Bales, B. L.; Meyer, M.; Smith, S.; Peric, M., EPR Line Shifts and Line Shape Changes Due to Spin Exchange of Nitroxide-Free Radicals in Liquids 6. Separating Line Broadening due to Spin Exchange and Dipolar Interactions. *J. Phys. Chem. A* **2009,** *113*, 4930-4940.
11. Bales, B. L.; Peric, M.; Dragutan, I., EPR Line Shifts and Line Shape Changes Due to Spin Exchange of Nitroxide Free Radicals in Liquids 3. Extension to Five Hyperfine Lines. Additional Line Shifts Due to Re-encounters. *J. Phys. Chem. A* **2003,** *107*, 9086-9098.
12. Bales, B. L.; Meyer, M.; Smith, S.; Peric, M., EPR Line Shifts and Line Shape Changes Due to Spin Exchange of Nitroxide-Free Radicals in Liquids 4. Test of a Method to Measure Re-encounter Rates in Liquids Employing ^{15}N and ^{14}N Nitroxide Spin Probes. *J. Phys. Chem. A* **2008,** *112*, 2177-2181.
13. Kurban, M. R.; Peric, M.; Bales, B. L., Nitroxide spin exchange due to re-encounter collisions in a series of *n*-alkanes. *J. Chem. Phys.* **2008,** *129*, 064501-1 - 064501-10.
14. Bales, B. L.; Harris, F. L.; Peric, M.; Peric, M., EPR Line Shifts and Line Shape Changes Due to Spin Exchange of Nitroxide-Free Radicals in Liquids 7. Singly Charged Surfactant Nitroxide. *J. Phys. Chem. A* **2009,** *113*, 9295-9303.
15. Kirste, B.; Kurreck, H.; Sordo, M., Syntheses and ENDOR Studies of Selectively Deuterated Galvinoxyl Radicals. Complete Determination of the 13C Hyperfine Coupling Constants of Coppinger's Radical. *Chem. Ber.* **1985,** *118*, 1782-1797.
16. Türke, M. T.; Parigi, G.; Luchinat, C.; Bennati, M., Overhauser DNP with 15N labelled Frémy's salt at 0.35 Tesla. *Phys. Chem. Chem. Phys.* **2012,** *14*, 502-510.
17. Türke, M. T.; Bennati, M., Comparison of Overhauser DNP at 0.34 and 3.4 T with Fremy's Salt. *Appl. Magn. Reson.* **2012,** *43*, 129-138.
18. Kurzbach, D.; Kattnig, D. R.; Zhang, B.; Schlüter, A. D.; Hinderberger, D., Loading and release capabilities of charged dendronized polymers revealed by EPR spectroscopy. *Chem. Sci.* **2012,** *3*, 2550-2558.

19. Gafurov, M.; Denysenkov, V.; Prandolini, M. J.; Prisner, T. F., Temperature Dependence of the Proton Overhauser DNP Enhancements on Aqueous Solutions of Fremy's Salt Measured in a Magnetic Field of 9.2 T. *Appl. Magn. Reson.* **2012,** *43*, 119-128.
20. Rozantsev, E. G., *Free Nitroxyl Radicals*. Plenum Press: New York-London, 1970.
21. *Handbook of Preparative Inorganic Chemistry*. 2nd ed.; Academic Press: New York-London, 1963; Vol. 1.
22. Bakirov, M. M.; Salikhov, K. M.; Peric , M.; Schwartz, R. N.; Bales, B. L., A Simple, Accurate Method to Determine the Effective Value of the Magnetic Induction of the Microwave Field from the Continuous Saturation of EPR Spectra of Fremy's Salt Solutions. Representative values of T_1. *Appl. Magn. Reson.* **2019,** *50*, 919-942.
23. Kooser, R. G.; Volland, W. V.; Freed, J. H., ESR Relaxation Sudies on Orbitally Degenerate Free Radicals. I. Benzene Anion and Tropenyl. *J. Chem. Phys.* **1969,** *50*, 5243-5257.
24. Bakirov, M. M.; Khairuzhdinov, I. T.; Salikhov, K. M.; Schwartz, R. N.; Bales, B. L., The Effect of Power Saturation on the Line Shapes of Nitroxide Spin Probes Under the Influence of Spin-Exchange and Dipole–Dipole Interactions Studied by CW EPR. *Appl. Magn. Reson.* **2022,** *53*, 1275-1350.
25. Bakirov, M. M.; Khairutdinov, I. T.; Schwartz, R. N.; Peric, M.; Bales, B. L., The Dobryakov–Lebedev Relation Extended to Partially Resolved EPR Spectra. *Appl. Magn. Reson.* **2021**.
26. Bales, B. L.; Bakirov, M. M.; Galeev, R. T.; Kirilyuk, I. A.; Kokorin, A. I.; Salikhov, K. M., The Current State of Measuring Bimolecular Spin Exchange Rates by the EPR Spectral Manifestations of the Exchange and Dipole-dipole interactions in Dilute Solutions of Nitroxide Free Radicals with Proton Hyperfine Structure. *Appl. Magn. Reson.* **2017,** *48*, 1399-1445.
27. Salikhov, K. M., *Fundamentals of Spin Exchange. Story of a Paradigm Shift*. Springer: Switzerland, 2019; p 265.
28. Bales, B. L.; Peric, M., EPR Line Shifts and Line Shape Changes Due to Spin Exchange Between Nitroxide Free Radicals in Liquids 10. Spin-Exchange Frequencies of the Order of the Nitrogen Hyperfine Interaction: A Hypothesis. *Appl. Magn. Reson.* **2017,** *48* (2), 175-200.